Zoology 158 (2023) 126091

Contents lists available at ScienceDirect

Zoology

journal homepage: www.elsevier.com/locate/zool

The prokaryotic community of *Chondrosia reniformis* Nardo, 1847: from diversity to mercury detection

Camilla Roveta [a,*], Barbara Calcinai [a], Federico Girolametti [b], Joana Fernandes Couceiro [c,d], Stefania Puce [a,1], Anna Annibaldi [a,1], Rodrigo Costa [c,d,e,1]

[a] Department of Life and Environmental Sciences, Università Politecnica delle Marche, Via Brecce Bianche, 60131 Ancona, Italy
[b] Department of Industrial Engineering and Mathematical Sciences, Università Politecnica delle Marche, Via Brecce Bianche, 60131 Ancona, Italy
[c] Institute for Bioengineering and Biosciences, Instituto Superior Técnico, Universidade de Lisboa, Av. Rovisco Pais 1, 1049-001 Lisboa, Portugal
[d] Associate Laboratory i4HB—Institute for Health and Bioeconomy at Instituto Superior Técnico, Universidade de Lisboa, Av. Rovisco Pais, 1049-001 Lisboa, Portugal
[e] Centre of Marine Sciences (CCMAR), University of Algarve, Portugal

ARTICLE INFO

Keywords:
Porifera
Metagenomics
Biomonitors
Atlantic Ocean

ABSTRACT

Microbial communities inhabiting sponges are known to take part in many metabolic pathways, including nutrient cycles, and possibly also in the bioaccumulation of trace elements (TEs). Here, we used high-throughput, Illumina sequencing of 16S rRNA genes to characterize the prokaryotic communities present in the cortex and choanosome, respectively the external and internal body region of *Chondrosia reniformis*, and in the surrounding seawater. Furthermore, we estimated the total mercury content (THg) in these body regions of the sponge and in the corresponding microbial cell pellets. Fifteen prokaryotic phyla were detected in association with *C. reniformis*, 13 belonging to the domain Bacteria and two to the Archaea. No significant differences between the prokaryotic community composition of the two regions were found. Three lineages of ammonium-oxidizing organisms (*Cenarchaeum symbiosum*, *Nitrosopumilus maritimus*, and *Nitrosococcus* sp.) co-dominated the prokaryotic community, suggesting ammonium oxidation/nitrification as a key metabolic pathway within the microbiome of *C. reniformis*. In the sponge fractions, higher THg levels were found in the choanosome compared to the cortex. In contrast, comparable THg levels found in the microbial pellets obtained from both regions were significantly lower than those observed in the corresponding sponge fractions. Our work provides new insights into the prokaryotic communities and TEs distribution in different body parts of a model organism relevant for marine conservation and biotechnology. In this sense, this study paves the way for scientists to deepen the possible application of sponges not only as bioindicators, but also as bioremediation tools of metal polluted environments.

1. Introduction

Microbes form complex relationships with most organisms, ranging from humans to invertebrates and plants (Thomas et al., 2016), with highly specialized reciprocal interactions, generally resulting in mutual benefits for both parties (Nyholm and McFall-Ngai, 2004; Schmitt et al., 2007). However, the diversity and highly dynamic nature of microbiomes make the understanding of the evolutionary and ecological drivers of symbiont composition challenging, as well as the possible roles played by the host-associated microbiota, which often result from multiple and interconnecting metabolic processes (Thomas et al., 2016).

Marine invertebrates, including clams, corals, mussels, sponges, seasquirts, and worms, are characterized by the presence of complex communities of microorganisms composing the associated microbiota (Thompson et al., 2021), generally hosted in their tissues, where nutrient cycling and host-microbe metabolite exchange take place (Schmitt et al., 2007). Sponges are sedentary filter-feeders, whose microbiome can be acquired horizontally from the seawater and vertically from parental sponges to offspring (de Oliveira et al., 2020). In many species, the sponge microbiome may be composed of up to 10^8–10^{10} cells g^{-1} of sponge wet weight and is largely dominated by prokaryotic species. Such sponges are usually referred to as

* Corresponding author.
E-mail address: c.roveta@staff.univm.it (C. Roveta).
[1] Equally contributing authors

https://doi.org/10.1016/j.zool.2023.126091
Received 10 June 2022; Received in revised form 21 February 2023; Accepted 16 March 2023
Available online 22 March 2023

"bacteriosponges" or "high microbial abundance" (HMA) sponges, in contrast to "low microbial abundance" (LMA) sponges, which possess microbial densities similar to those of the surrounding seawater (10^6 cells g^{-1}) (Vacelet and Donadey, 1977; Schmitt et al., 2007; Gloeckner et al., 2014).

Sponges are reservoirs of microbial genetic diversity, and the often-reported taxonomic diversification among so-far uncultivated sponge symbionts is suggestive of metabolic novelties (Hardoim et al., 2014). Metabarcoding studies based on 16S rRNA gene amplicon sequencing showed how sponges not only present interspecific variability in the structure of their associated microbial communities, but also intraspecific variability between individuals of the same species collected in different localities (Hardoim et al., 2012). These patterns can be related to many factors, such as host-derived nutrients, chemical-physical parameters of the water (e.g., pH) and host characteristics (e.g., immune response), determining the composition and structure of symbiont communities over time and space (Thomas et al., 2016). Only 1–14% of the total sponge bacterial community has been estimated to be cultivatable (Hardoim et al., 2014). In fact, culturable symbionts usually correspond to low abundance ("rare") taxa within this complex microbial consortium (Hardoim et al. 2014; Karimi et al., 2019), limiting our knowledge of the functional roles played by most of the sponge symbionts, which remain uncultivated (Karimi et al., 2019).

Sponges can filter large volumes of water (processing up to 35 ml min^{-1} (cm sponge)$^{-3}$) (Weisz et al., 2008), together with food particles and many different compounds, which are present in the water column both as dissolved and particulate organic and inorganic matter (Berthet et al., 2005; Selvin et al., 2009; Batista et al., 2014). Among these compounds, contaminants (as hydrocarbons, organochlorinated compounds, trace elements, etc.) are largely collected. Various studies demonstrated that sponges could present detectable concentrations of trace elements (TEs), and bioaccumulate these pollutants in their mesohyl (e.g., Perez et al., 2004, 2005; Cebrian et al., 2006; Batista et al., 2014), even though the dynamics regulating the bioaccumulation process are still largely unknown (Li et al., 2022). Thus, sponges are considered suitable bioindicators of environmental pollution, and they have been recommended by various European Directives, such as the Water Framework Directive (WFD, 2000/60/EC) and the Marine Strategy Framework Directive (MSFD, 2008/56/EC) as possible monitors of TEs contamination. In addition, since the microbiome plays a fundamental role in the sponge metabolism, it has been suggested it can also actively participate in the bioaccumulation process, and many bacteria have been found to be resistant to various antibiotics and pollutants, including persistent organic pollutants and TEs (e.g., Cd, Co, Cu, Hg, Ni, Pb, Zn, and their organic compounds) (e.g., Selvin et al., 2009; Versluis et al., 2016; Rodriguez Jimenez et al., 2021). For these reasons, sponges and their associated bacteria have been also proposed as valid bioremediation tools (Santos-Gandelman et al., 2014a, 2014b).

Chondrosia reniformis Nardo, 1847 is a typical cushion-shaped, Atlanto-Mediterranean demosponge usually living in the shallow coastal waters (0–50 m) (Wilkinson and Vacelet, 1979; Lazoski et al., 2001). The sponge possesses profuse collagen fibres, which confer the organism a high body plasticity (Bonasoro et al., 2001). The structure of *C. reniformis* consists of two distinct body regions: a cortical zone, named ectosome or cortex, composed by flattened pinacocytes and densely packed interwoven collagenous fibers, and an internal zone, named choanosome, which contains the choanocyte chambers (Bavestrello et al., 1988, 1998a, 1998b; Cerrano et al., 1999). Lacking a siliceous skeleton, *C. reniformis* reinforces its body incorporating large amounts of foreign material: the cortex incorporates only siliceous particles, while the choanosome allows the attachment of any kind of mineral (Bavestrello et al., 1998a). *C. reniformis* is known to be the source of several secondary metabolites, and therefore is commonly reared for in situ or aquaria studies. In fact, the species represents an important source of collagen and other molecules, such as chondrosin, a newly discovered protein with anti-tumoral activity (Pozzolini et al., 2012, 2015, 2016, 2018; Scarfì et al., 2020). Moreover, *C. reniformis* was already identified as a suitable bioindicator of TEs pollution, reflecting more accurately the contamination levels of a specific location compared to other sponge species (Perez et al., 2004; Cebrian et al., 2007; Roveta et al., 2020, 2022).

Since *C. reniformis* presents two distinct body regions, with a very different physical-chemical architecture (Bavestrello et al., 1998a, 1998b; Cerrano et al., 1999), and considering that the distribution of the TEs within sponges is often heterogeneous, being possibly microbial-mediated (Padovan et al., 2012; Batista et al., 2014), we hypothesized that cortex and choanosome can display a different concentration of TEs related to a different microbial community composition. In this context, here we describe the prokaryotic community and mercury (Hg) content of *C. reniformis* samples collected in Faro (Portugal, Atlantic Ocean). The possible presence of mercury (Hg) in microbial cell pellets extracted from the two body regions of the sponge (cortex and choanosome) was explored and compared with the total mercury content (THg) estimated directly in the sponge fraction representing both body regions. Additionally, we identified the microbial taxa present in the extracted cell pellets using next-generation sequencing of 16S rRNA genes. This study contributes to a better knowledge of TEs distribution in sponges and of the prokaryotic communities associated with the cortex and choanosome layers of the model organism *C. reniformis*.

2. Materials and methods

2.1. Samples collection and processing

Eleven samples of *Chondrosia reniformis* were collected into sterile bags by SCUBA diving at ~18 m depth at offshore Faro beach, Algarve, Portugal ("Pedra da Greta": 36°58'47.2" N, 07°59'20.8" E), in June 2021. Samples were collected at least 3 m apart from each other, to avoid clones, and placed in 3 L plastic bags (type Ziploc®) filled with surrounding seawater. The collected sponge samples were of similar size to avoid possible differences in sponge age, since different THg levels could be related to this factor (Cebrian et al., 2007; Orani et al., 2020; Roveta et al., 2022). Together with sponges, four samples of seawater (3 L each) were also collected in separate Ziploc plastic bags, 1.5 m above the bottom. All samples were transported to the Environmental Sample Processing Facility of the Centre of Marine Sciences (Faro, Portugal) in a cool box within 1.5 h post sampling and processed immediately.

Sponge samples were cleaned of rock reseals, washed with sterile seawater to remove planktonic or loosely associated microorganisms, following Thomas et al. (2016). Since *C. reniformis* is characterized by two body regions, the cortex and the choanosome (Bavestrello et al., 1998a, 1998b), each region was separated for each sample, using a decontaminated knife (see Illuminati et al., 2016 for the decontamination procedure). After separation each sub-sample was labelled with the following codes: CrI (*C. reniformis* internal, referring to the choanosome), and CrE (*C. reniformis* external, referring to the cortex), followed by sequential numbers. Seawater samples were instead labelled as W followed by sequential numbers. Microbial cell pellets were obtained from 10 g of weighted material (from each sub-sample) using a differential centrifugation protocol applied to sponge-derived homogenates as described by Hardoim et al. (2014). Firstly, due to the hardness of the sponge given by collagenous fibres, each region of *C. reniformis* was mixed with a blender in sterile Ca^{2+} and Mg^{2+} free artificial seawater (CMFASW: 27 g L^{-1} NaCl, 1 g L^{-1} NaSO4, 0.8 g L^{-1} KCl and 0.18 g L^{-1} NaHCO3, 1 g of sponge per 4 ml CMFASW w/v) and then further homogenized using a sterile mortar and pestle. Homogenates were thereafter centrifuged for 2 min at 500 xg, and supernatants containing the microbial cells released from the sponge matrix, characterized by smaller cell sizes than those of the cells enriched in the sponge fraction, were transferred into new centrifuge tubes, and subjected to a final centrifugation step for 30 min at 10,000 xg. The applied protocol allows to obtain a pellet enriched in microbial cells with negligible

contamination of sponge cells, as estimated using shotgun metagenome sequencing (less than 2% of host-derived reads in the microbial cell pellets) (Karimi et al., 2017). The sponge fraction and the derived microbial cell pellet obtained for each specimen were then used to determine the THg content in both internal and external parts of the *C. reniformis* body.

Additional 2.5 g of four of the same *C. reniformis* samples were subjected to the protocol described above for the retrieval of microbial cell pellets. These microbial pellets were then used for total community microbial DNA extraction for the characterization of the prokaryotic communities associated with the species (see below). Briefly, this methodology enables high-quality metagenomic DNA yields suitable for molecular analyses of the marine sponge microbiome, leading to comprehensive coverage of the diversity of sponge-associated prokaryotes (Fieseler et al., 2006), also when compared with direct DNA extractions from bulk sponge samples (Hardoim et al., 2014). DNA extraction from microbial cell pellets was, therefore, the method of choice in this study to analyse the prokaryotic community associated with *C. reniformis* because of the particularly hard consistency of this sponge species. Finally, three out of four seawater samples were filtered using 0.22 μM nitrocellulose membrane filters (Millipore, Billerica, MA, USA; 47 mm) using a vacuum pump, to collect the water microbiota. All the obtained material was then stored at −80°C until further analysis.

2.2. DNA extraction and 16S rRNA gene sequencing from Chondrosia reniformis and seawater samples

The microbial pellets of each body region and filters were subjected to total community DNA extraction using the Power Soil® DNA Isolation Kit (Qiagen, USA) according to the manufacturer's protocol. One DNA extraction was carried out without any sample to serve as a negative control. Before the extraction, water filters were aseptically cut into small pieces. Each sample was then transferred to a lysing matrix tube provided by the kit and subjected to bead-beating three times for 1 min (30.0 frequency) with a Mixer Mill MM 400 to improve submersion and contact between cells and lysing buffer. Metagenomic DNA yields and integrity were examined under ultraviolet (UV) light after standard agarose gel electrophoresis procedures, while the concentration of the DNA samples was quantified using a NanoDrop spectrophotometer (ThermoFischer Scientific).

Taxonomic profiling of bacterial communities was performed via high-throughput sequencing of 16S rRNA gene amplicons obtained by PCR from the metagenomic DNA samples. PCR amplification and sequencing of 16S rRNA gene amplicons was performed at MR DNA (www.mrdnalab.com, Shallowater, TX, USA). The primers used were the updated Earth Microbiome Project (EMP) primers 515F (5'-GTG YCA GCM GCC GCG GTAA-3') (Parada et al., 2016) and 806RB (5'-GGA CTA CNV GGG TWT CTA AT-3') (Apprill et al., 2015). Firstly, a 30–35-cycle PCR was used to amplify the V4 hypervariable region (515−806) of the 16S rRNA gene, using the HotStarTaq Plus Master Mix Kit (Qiagen, USA). The conditions for the PCR were as follows: a first step of 5 min at 95°C, followed by 30–35 cycles of 30 s at 95 °C, 40 s at 53 °C and 1 min at 72 °C, after which there was one final elongation step of 10 min at 72°C. PCR products were checked in a 2% agarose gel under UV light to determine whether the amplification was successful, including proper monitoring of negative controls from which no amplicons were observed. After amplification, the samples were multiplexed using unique dual indexing, pooled together and later purified using calibrated Ampure XP beads. Afterwards, the pooled and purified PCR products were used to prepare an Illumina DNA library, and sequencing was performed on a MiSeq platform following the manufacturer's guidelines. During sequencing, an average 20,000 paired-end sequences, per sample, were generated.

2.3. Total mercury content analysis

The sponge fraction obtained from the cortex and choanosome of the eleven processed samples was lyophilized (Edwards EF4 modulyo, Crawley, Sussex, England), minced, homogenized, and divided in aliquots of about 0.02 g each. The microbial pellet was instead centrifuged before the analysis at 1000 *rpm* for 1 min to remove water residuals. Hg analyses were performed at the Department of Life and Environmental Sciences of the Polytechnic University of Marche, using a direct mercury analyser (DMA-1) as reported in Roveta et al. (2020).

Both filtered and non-filtered seawater were diluted with ultrapure grade HCl 2% (v/v), and then analysed with a AFS Titan 8220 spectrofluorometer (Fulltech Instruments, Rome, Italy). Argon 5.0 (99.999% purity) was used as a gas carrier and ultrapure grade HCl 5% (v/v) was used as the sample carrier. $NaBH_4$ 0.05% in NaOH 0.4% (m/v) was used as reductant agent to produce Hg hydrides. Instrumental parameters are reported in Table S1 (Supplementary Material).

All measurements were replicated at least 4 times. A calibration curve was constructed to quantify THg content. The analytical accuracy is routinely checked using the appropriate Certified Reference Materials (CRMs), in this study DORM-2 and MESS-2 (National Research Council Canada, Ottawa, Canada). Details are reported in Table S2 of the Supplementary Material.

2.4. Data treatment and analysis

2.4.1. Bacterial community diversity and composition

In total, 313,846 raw 16S rRNA (V4 region) gene sequence reads were obtained and subjected to quality filtering and processing with the MR DNA (www.mrdnalab.com) taxonomic analysis pipeline, a suite of proprietary, open-source software packages which integrates Usearch v11 (https://drive5.com/usearch/manual/; Edgar, 2010). Firstly, primers were removed from sequences, and sequences below 150 bp or with ambiguous base calls were filtered out. Subsequent denoising and dereplication of the sequences consisted of identifying and removing reads with sequencing or PCR point errors (using a maximum expected error threshold of 1.0) and removing chimeric sequences with the unoise3 command (https://www.drive5.com/usearch/manual/cmd_unoise3.html), which is an implementation of the UNOISE algorithm (Edgar and Flyvbjerg, 2015).

After denoising and dereplicating the sequences, zero-radius Operational Taxonomic Units (zOTUs), or Amplicon Sequence Variants, were generated and integrated into a zOTU abundance table, containing counts of each zOTU per sample, using the otutab command (https://www.drive5.com/usearch/manual/cmd_otutab.html) within Usearch v11, and taxonomically classified using BLASTn against a curated database derived from NCBI (www.ncbi.nlm.nih.gov). Briefly, 16S rRNA gene reads possessing 100% nucleotide sequence homology are categorized into the same zOTU. Prior to downstream analyses, zOTUs classified as Eukaryota, chloroplasts or mitochondria were removed from the obtained zOTU abundance table. The final analytical dataset comprised 303,732 16S rRNA gene reads sorted into 448 prokaryotic zOTUs, 17 belonging to the domain Archaea and 431 to the domain Bacteria (Table S3, Supplementary Material).

For alpha-diversity analyses, the dataset was normalized by rarefaction to 23,477 reads per sample (corresponding to sample W3 which had the lowest number of reads), and the rarefied dataset was then used for the determination of observed species richness, estimated species richness (Chao1 index) and diversity (Shannon's index). Rarefaction and diversity measures were carried out using the R package *phyloseq* (McMurdie and Holmes, 2013). To test for possible differences in the alpha-diversity of W, CrE and CrI, a one-way ANOVA test was applied. The normality of the data was tested with a Shapiro-Wilk's test and the homogeneity of the variance with a Levene's test. In case of statistically significant differences, the Tukey's test was performed. Statistical tests were performed using R packages *car*, *stats* and *rstatix* (Fox and

Weisberg, 2019; Kassambara, 2021; R Core Team, 2021).

To assess the prokaryotic community composition of each sample at phylum, class and genus levels, relative abundance data (percentages, non-rarefied) were used (Table S4, Supplementary Material). To improve the readability of taxonomy barplots, low abundance taxa (taxa below 1% relative abundance for the order plot and below 0.5% for the phylum and genus plots) were merged in a category called "Others". Plots were created using R packages *phyloseq*, *plyr* and *ggplot2* (Wickham, 2011; McMurdie and Holmes, 2013; Wickham, 2016). One-way ANOVAs followed by Tukey's post-hoc tests were used to test for differences in the relative abundance of the most dominant phyla across sample categories (W, CrI, CrE).

The prokaryotic community structure was also investigated by means of multivariate analysis. zOTU data (non-rarefied) were Hellinger-transformed and the Bray-Curtis dissimilarities calculated from the Hellinger-transformed OTU-data table using the *vegan* package for R (Oksanen et al., 2020). The resulting dissimilarity matrix was then used as input in a Principal Coordinates Analysis (PCoA) of the samples based on their zOTU profiles. To complement the result given by the PCoA, an analysis of Similarity Percentages (SIMPER) was carried out with the free software PAST (PAleontological STatistics, version 4.02; Hammer et al., 2001) to rank the zOTUs contributing the most to community dissimilarities among sample groups. SIMPER was performed considering all sample groups together and the resulting top 15 zOTUs were plotted as "species data" on the PCoA graph. To investigate whether there was a significant difference between sample groups (W, CrI and CrE), data were analysed with Permutational Analysis of Variance (PERMANOVA) (Anderson, 2001), using a Bray-Curtis dissimilarity matrix, with 9999 permutations. *A posteriori* pairwise comparisons were conducted in case of significant differences. Permutational analysis of multivariate dispersions (PERMDISP) was used to test the homogeneity of samples dispersion from their group centroids (Anderson et al., 2008). These analyses were carried out using PRIMER 7.0.20 (Clarke and Gorley, 2015) with the add-on PERMANOVA+ (Anderson et al., 2008). All statistical analyses were done with a 95% confidence level ($p < 0.05$).

2.4.2. Total mercury content

THg content in sponge samples and associated microbiota was expressed in mg kg^{-1} dry weight (d.w.), while seawater data (filtered and unfiltered) were expressed in ng L^{-1}. To assess the capability of both sponge fractions and microbiota to bioconcentrate Hg, the bioconcentration factor (BAF) was calculated using the formula: $BAF_{sponge} = THg_{sponge}/THg_{filtered\ water}$ and $BAF_{microbiota} = THg_{microbiota}/THg_{filtered\ water}$.

To test for possible differences in the THg content between filtered and unfiltered seawater samples, a one-taled Student *t* test was carried out. One-way ANOVA (with Tuckey's post-hoc) was performed to test for differences in THg content (among samples, sponge fraction and microbial pellet) and BAF values. In case of non-normality or heteroscedasticity, non-parametric Kruskal-Wallis analysis of variance was applied and, if statistically significant differences were found, the Dunn's post-hoc comparison was performed. Statistical tests were performed using R packages *car*, *stats* and *rstatix* (Fox and Weisberg, 2019; Kassambara, 2021; R Core Team, 2021), and with a 95% confidence level ($p < 0.05$).

3. Results

3.1. Alpha-diversity analyses

Alpha-diversity (species richness and Shannon's diversity) in seawater and in *Chondrosia reniformis* was explored using the rarefied dataset. The observed number of zOTUs was significantly higher in seawater compared to CrE and CrI samples (Tukey's test, $p < 0.05$) (Fig. 1 A). The estimated species richness (Chao1) was slightly higher than the observed richness in all samples, except for samples W3, CrI1 and CrE1 in which the two values were almost overlapping (Fig. 1 A). No differences among sample groups were found for Chao1 (ANOVA, $p > 0.05$), even though the seawater showed the highest values of estimated richness (Fig. 1 A). Shannon diversity indices were significantly higher for seawater than in CrI and CrE samples (Tuckey's test, $p < 0.05$) (Fig. 1B).

In general, between the two body regions of *C. reniformis*, CrI samples exhibited higher observed and Chao1 richness, and a lower Shannon Diversity compared to CrE samples (Fig. 1), but no statistical differences were recorded (Tuckey's test, $p > 0.05$).

3.2. Prokaryotic community composition

Proteobacteria, Nitrososphaerota (formerly Thaumarchaeota), Acidobacteria, Bacteroidetes, Chloroflexi (in this order) were the dominant phyla in the entire dataset (Fig. 2 A), with their relative abundance changing significantly among categories (one-way ANOVA, $p < 0.05$), and especially between the seawater and the two body regions of *C. reniformis* (Tuckey's test, $p < 0.05$). Overall, Proteobacteria was the most abundant phylum: in seawater samples, it accounted for almost the 75% of the dataset, while in CrI and CrE samples, it represented about the 50% of the entire microbial community (Fig. 2 A). Another phylum with a significative relative abundance in water samples was Bacteroidetes, almost reaching 20%, while lower values (~7%) were represented by Cyanobacteria. *C. reniformis* prokaryotic

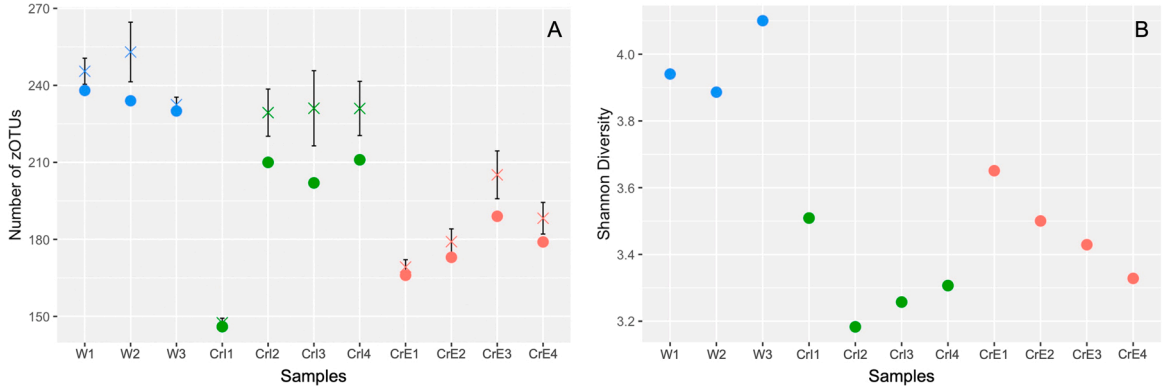

Fig. 1. Alpha diversity measures estimated for prokaryotic communities in *Chondrosia reniformis* and surrounding seawater. (A) Observed (•) and Chao-estimated (×) zOTU richness per sample. (B) zOTU diversity per sample estimated with the Shannon diversity index. Alpha diversity measures were calculated using the rarefied dataset. W = water; CrI = *C. reniformis* internal, referring to the choanosome; CrE = *C. reniformis* external, referring to the cortex. Sequential numbers represent replicate samples obtained for seawater (1–3) and *Chondrosia reniformis* (1–4).

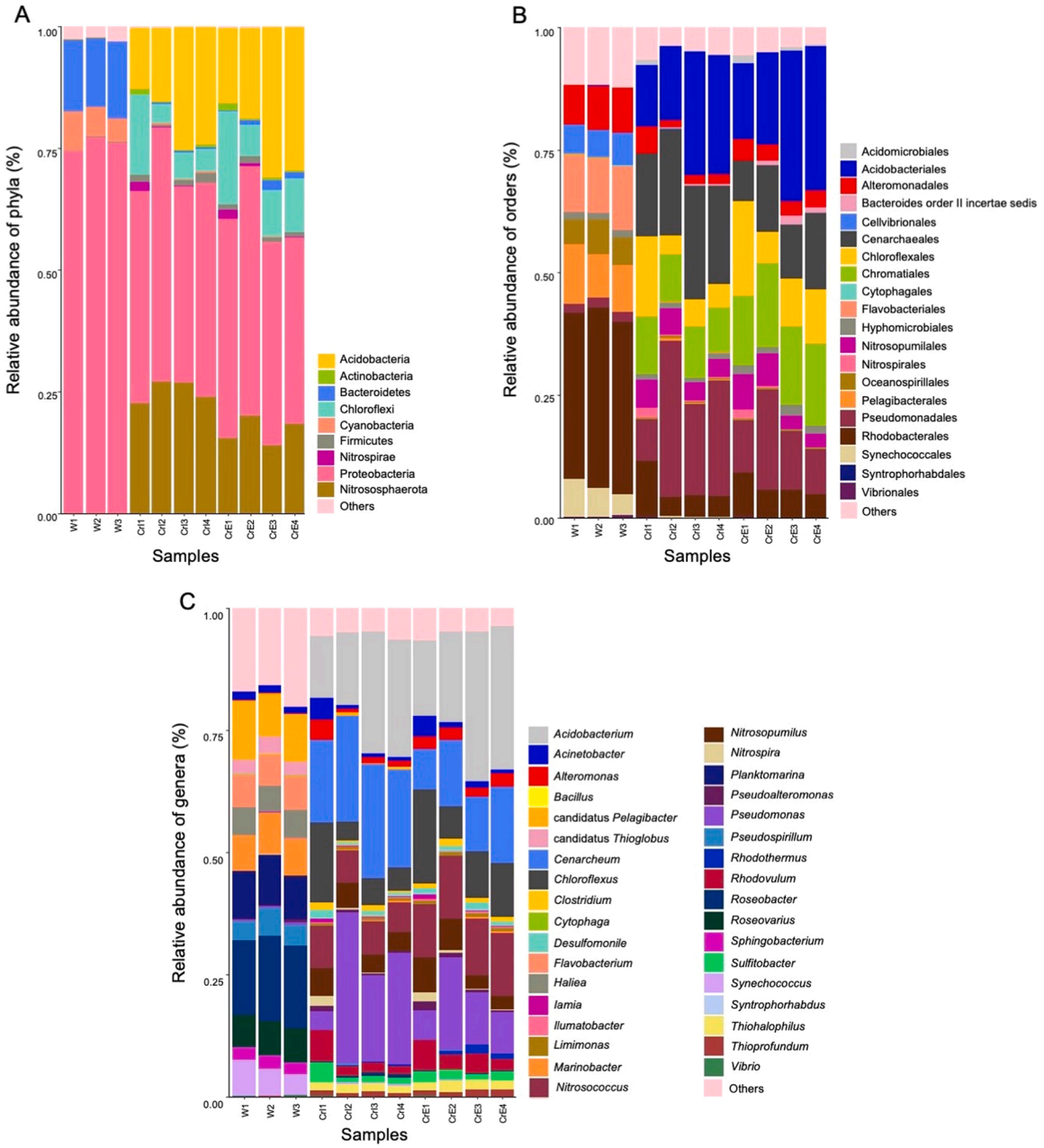

Fig. 2. Taxonomic composition of prokaryotic communities in *Chondrosia reniformis* and seawater. (A) Phylum, (B) Order and (C) Genus level taxonomies are shown, using taxon relative abundances calculated from the non-rarefied zOTUs table (Table S4). Phyla and genera presenting relative abundances below 0.5 %, and orders presenting relative abundances below 1 % were joined under the category "Others". W = water; CrI = *C. reniformis* internal, referring to the choanosome; CrE = *C. reniformis* external, referring to the cortex. Sequential numbers represent replicate samples obtained for seawater (1−3) and *Chondrosia reniformis* (1−4). Taxonomy assignments were performed using the current NCBI nomenclature. The former archaeal phylum Thaumarchaeota is now validly published under the name Nitrososphaeorota. (For interpretation of the references to color in this figure legend, the reader is referred to the web version of this article)

community was also characterized by a high relative abundance of Nitrososphaerota (formerly Thaumarchaeota), an archaeal phylum representing about the 20–30% of the microbiota, and of Acidobacteria, ranging from 15% to 40% of the reads in CrE and CrI datasets (Fig. 2 A). The phylum Chloroflexi was also well represented, with relative abundances around 10%; lower values were instead recorded for Actinobacteria, Bacteroidetes, Firmicutes and Nitrospirae (< 5%) (Fig. 2 A).

At the order-level, both CrE and CrI presented a highly diversified community, with the highest relative abundance reached by the archaeal order Cenarchaeales, and by the bacterial orders Acidobacteriales and Pseudomonales, each representing ~25% of the total reads (Fig. 2B). Other orders, such as Alteromonadales, Chloroflexales, Chromatiales, Nitrosopumilales and Rhodobacterales, also showed considerable relative abundances in CrE and CrI samples (Fig. 2B). Order Rhodobacterales was dominant in all seawater samples, representing about 45% of the prokaryotic community, while a lower contribution was given by Alteromonadales, Cellvibrionales, Flavobacteriales, Oceanospirillales, Pelagibacterales and Synechoccocales (Fig. 2B).

At genus-level seawater samples were mostly dominated by *Roseobacter* (~30%), followed by *Flavobacterium*, *Marinobacter*, candidatus *Pelagibacter*, *Planktomarina*, *Roseovarius* and *Synechococcus,* contributing between 6% and 12% (Fig. 2 C), while CrE and CrI samples were dominated by *Pseudomonas*, *Cenarchaeum* and *Acidobacterium*, each representing ~20% of the prokaryotic community, followed by

Chloroflexus, *Nitrososcoccus* and *Nitrosopumilus* (Fig. 2 C).

3.3. Beta-diversity analysis

The PCoA revealed a clear separation between seawater and *C. reniformis* samples (Fig. 3). CrI and CrE samples formed two single and separate clusters, with the exception of CrI1 and CrE1, which formed a separate group from the other samples (Fig. 3). The PERMANOVA showed statistical differences across sample groups ($p < 0.05$) (Table 1), with the pairwise comparison highlighting significant differences only between seawater samples and both regions of *C. reniformis'* body ($p < 0.05$), while no differences were found between CrI and CrE ($p > 0.5$) (Table 2). Even though the PERMDISP test indicated a similar average dispersion in each samples' groups ($p > 0.5$) (Table 3), particulalry between CrI and CrE samples, making differences in dispersion within groups not significant ($F_{2,8} = 3.4322$; $p = 0.3295$), an additional PERMANOVA test without considering sample 1 (possibly seen as an outlier) was performed. Also in this case, the analysis did not find statistically significant differences between the cortex and choanosome of the studied sponge regarding the structure of their prokaryotic communities at the zOTU level (Table S5). In spite of this, using SIMPER we were able to find a few zOTUs more characteristic of one body region or the other. This was the case of zOTU3 (*Pseudomonas* sp.) and zOTU1 (*Cenarchaeum symbiosium*), found to possess higher relative abundances in CRI than in CRE, and of zOTU6 (*Nitrosococcus* sp.), possessing higher relative abundance in CRE than in CRI (Table S4).

In this ordination plot, the fifteen most differentiating zOTUs were also displayed, showing their effect and contribution to the dissimilarity between samples. For instance, zOTUs classified as *Marinobacter*, candidatus *Pelagibacter, Planktomarina, Roseobacter, Roseovarius, Pseudospirillum* and *Synechococcus* were associated with water samples (Fig. 3). Associated to *C. reniformis* samples were zOTUs affiliated with the Archaea species *C. symbiosum* and *N. maritimus*, the bacterial genera *Chloroflexus, Nitrosococcus, Pseudomonas*, and zOTUs classified as *Acidobacterium* (Fig. 3).

Table 1
Results of the one-way PERMANOVA. Analysis of microbial community variation within samples' groups (water, *Chondrosia reniformis* internal choanosome and *C. reniformis* external cortex). df = degrees of freedom; SS = sum of squares; MS = mean squares; Pseudo-F = F-ratio; P (perm) = probability; Up = unique perms. Significant p-values ($p < 0.05$) are given in bold.

Source	df	SS	MS	Pseudo-F	P (perm)	Up
Samples	2	19,010	9504.8	38.09	**0.0027**	9697
Residuals	8	1996.4	249.55			
Total	10	21,006				

Table 2
Results of the a posteriori pairwise comparisons within samples' groups (water, *Chondrosia reniformis* internal choanosome and *C. reniformis* external cortex). t = t-test; P (perm) = probability; Up = unique perms. Significant p-values ($p < 0.05$) are given in bold. W = seawater; CrI = *Chondrosia reniformis* internal, referring to the choanosome; CrE = *C. reniformis* external, referring to the cortex.

Groups	t	P (perm)	Unique perms
W, CrI	7.51	**0.0279**	9936
W, CrE	9.55	**0.0288**	9908
CrI, CrE	1.01	0.4563	9916

Table 3
Results of the PERMDISP analysis within samples' groups (water, *Chondrosia reniformis* internal choanosome and *C. reniformis* external cortex). SE = standard error. W = seawater; CrI = *Chondrosia reniformis* internal, referring to the choanosome; CrE = *C. reniformis* external, referring to the cortex.

Group	Size	Average dispersion	SE
W	3	5.73	0.41
CrI	4	15.89	3.45
CrE	4	12.99	2.39

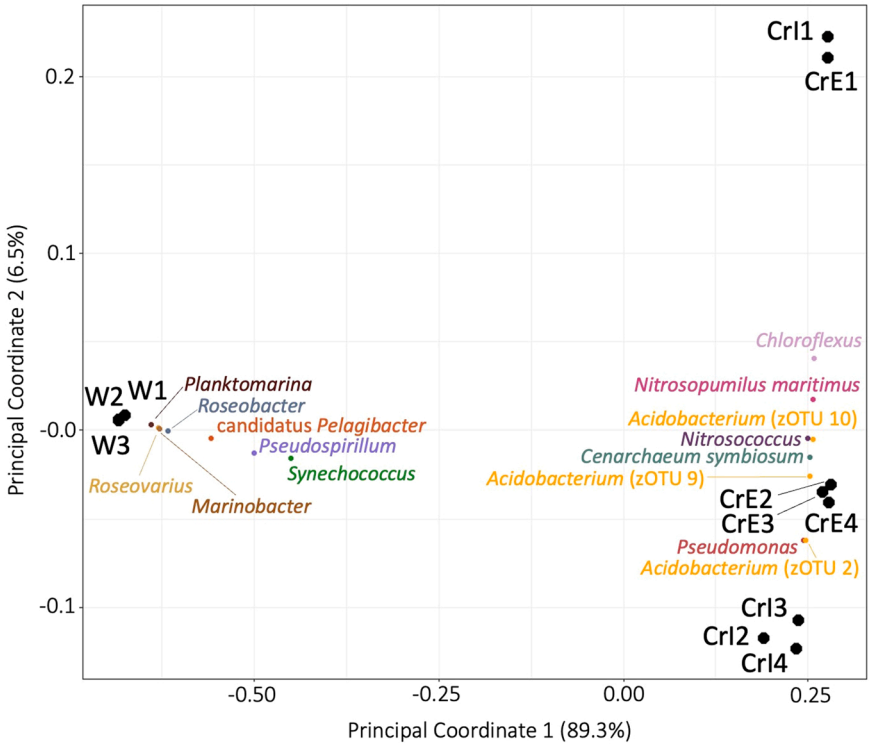

Fig. 3. Principal Coordinates Analysis (PCoA) of prokaryotic communities in *Chondrosia reniformis* and ambient seawater samples. Community ordination was based on a Bray-Curtis distance matrix calculated from Hellinger-transformed zOTU abundance data. The 15 zOTUs with higher contribution to the dissimilarity between sample groups (namely seawater, *C. reniformis* internal and *C. reniformis* external), as estimated using SIMPER, are plotted on the ordination diagram. The position of the zOTUs is a projection of their respective abundances in the space formed by the two principal coordinates. The closest the proximity of zOTUs to a given sample group, the highest the relative abundance of those zOTUs in that sample group. Samples are represented by black dots surrounded by their respective labels and zOTUs are marked as smaller, colored dots. Percentage values on each axis (Principal Coordinate) correspond to the amount of variance explained by that axis. W = water; CrI = *C. reniformis* internal, referring to the choanosome; CrE = *C. reniformis* external, referring to the cortex. Sequential numbers represent replicate samples obtained for seawater (1−3) and *Chondrosia reniformis* (1−4).

3.4. Total mercury content

THg levels in the unfiltered seawater samples were slightly higher (3.9 ± 1.9 ng L^{-1}) than in the filtered one (3.3 ± 1.4 ng L^{-1}) (Table 4), even though the Student *t* test did not highlight any significant differences between them ($p > 0.05$). In addition, the mean THg value recorded in the filters with the microbiome extracted from the seawater was nearly negligible, measuring 0.0034 ± 0.0008 mg kg^{-1} d.w. (Table 4).

No differences in the THg values among sponge samples were recorded (one-way ANOVA, $p > 0.05$), while significant differences were found between the two body regions (one-way ANOVA, $p < 0.05$), with higher values in CrI (0.70 ± 0.08 mg kg^{-1} d.w., ranging from 0.51 to 0.82 mg kg^{-1} d.w.) than in CrE (0.26 ± 0.07 mg kg^{-1} d.w., ranging from 0.15 to 0.41 mg kg^{-1} d.w.) (Table 4; Fig. 4). In the microbial pellet, the mean THg concentration in the microbiome extracted from CrI ranged from 0.06 to 0.12 mg kg^{-1} d.w. (0.08 ± 0.01 mg kg^{-1} d.w.) and the one extracted from CrE from 0.068 to 0.12 mg kg^{-1} d.w. (0.079 ± 0.02 mg kg^{-1} d.w.), resulting extremely similar (one-way ANOVA, $p > 0.05$) (Table 4; Fig. 4).

Clear differences were recorded between THg values of the sponge fraction and the extracted microbiome within both body regions (Kruskal-Wallis, $p < 0.05$). Higher THg values were found in both sponge fractions compared to the corresponding microbial pellet (Dunn's test, $p < 0.05$) (Fig. 4), with a ratio of 8:1 and 3:1 for CrI and CrE, respectively.

Similarly, BAF values were significantly higher in the choanosome than in the cortex (one-way ANOVA, $p < 0.05$), while no differences were recorded between the microbial pellet extracted from the two fractions (Kruskal-Wallis, $p > 0.05$) (Table 4). BAF values were also different between the sponge fraction and the extracted microbiota in both CrI and CrE (Kruskal-Wallis, $p < 0.05$), with higher values in the sponge.

4. Discussion

The current study describes the prokaryotic communities of the two body regions characterizing *Chondrosia reniformis*, the choanosome and the cortex. Among the 15 phyla detected, those belonging to domain Bacteria dominated the microbial community, mainly represented by Proteobacteria, Acidobacteria, Bacteroidetes and Chloroflexi, while two phyla belonging to domain Archaea, Euryarchaeota and Nitrososphaerota (formerly Thaumarchaeota), were also recorded. These observations are in line with previous studies on HMA sponges from both the Atlanto-Mediterranean region such as *Ircinia felix*, *Sarcotragus spinosulus, Spongia officinalis* and *Xestospongia muta* (e.g., Schmitt et al., 2012; Hardoim et al., 2012, 2014; Karimi et al., 2017) and other geographic locations, such as *Luffariella variabilis* and *Rhopaloeides odorabile* (e.g., Schmitt et al., 2012; Webster et al., 2013; Thomas et al., 2016). Specifically, the community profiles described here deepen our understanding about the prokaryotic community assembly in *C. reniformis*, owing to the higher resolution and more comprehensive nature of the molecular approach employed in comparison with earlier, taxon-specific studies (Manz et al. 2000; Ribes et al., 2012). Our 16S rRNA gene sequencing approach revealed three prokaryotic lineages, namely the archaea *Cenarchaeum symbiosum* and *Nitrosopumilus maritimus* and the Gammaproteobacterium *Nitrosococcus* sp., likely contributing to ammonium oxidation within *C. reniformis*, as demonstrated in other sponge species (e.g., Preston et al., 1996; Hallam et al., 2006; Feng et al., 2016). Additionally, using taxon-specific primers targeting the subunit A of the ammonium monooxygenase (*AmoA*) gene in a cloning-and-sequencing approach, Ribes et al. (2012) found evidence for the presence of ammonium-oxidizing Gammaproteobacteria in *C. reiniformis* specimens from the Montgrí Coast (Mediterranean Sea). In an earlier study, using widefield deconvolution epifluorescence microscopy combined with fluorescence in situ hybridization, Manz et al. (2000) used specific probes to localize sulfate-reducing Desulfovibrionaceae spp. (class Deltaproteobacteria, order Desulfovibrionales) within the *C. reniformis* mesohyl. They demonstrated that these rod-shaped bacteria tended to form small colonies around the channel system, surrounded by a large density of likely diverse, coccoid bacterial cells. Although we did not detect members of the Desulfovibrionaceae family in our samples, neither in the choanosome nor in the cortex, we report instead the enrichment of the sulfate-reducing family Desulfobacteraceae (class Deltaproteobacteria, order Desulfobacterales) in both body regions, suggesting functional convergence of the *C. reniformis* microbiome in key metabolic pathways (in this case, sulfate reduction). Differences in resolution and approach are the most likely reasons for some of the contrasting results observed between this and earlier studies. However, the fact that the specimens examined in each study come from different sites and marine provinces can also contribute to these outcomes, as it is known that intraspecific variability between individuals of the same species collected in different localities can occur (e.g., Hardoim et al., 2012; O'Connor-Sánchez et al., 2014; Griffiths et al., 2019; Easson et al., 2020).

Even though *C. reniformis* is characterized by a distinct texture and physical-chemical architecture which creates two distinct body regions (Bavestrello et al., 1988, 1995, 1998a, 1998b; Cerrano et al., 1999), in contrast to our hypothesis, no significant differences were recorded in the prokaryotic community structure between the cortex and the choanosome. Although it cannot be ruled out that bacterial taxa eventually involved in the process of Hg retention in the cortex and/or choanosome of *C. reniformis* could have possibly been missed because of the chosen methodology, centred on the analysis of metagenomic DNA extracted from microbial cell pellets obtained from both body regions (instead of DNA extracted directly from bulk sponge samples), this approach has been found to deliver robust coverage of the prokaryotic diversity in marine sponges (Fieseler et al., 2006; Hardoim et al., 2014). Moreover, the lack of sharp differences between prokaryotic community structures of the cortex and choanosome of *C. reniformis* is congruent with the similar levels of THg estimated for the microbial cell pellets from both body regions. Therefore, even though a few individual zOTUs have been identified as more characteristic of the choanosome (e.g., *Pseudomonas* sp. and *Cenarchaeum symbiosium*) and cortex (e.g., *Nitrosococcus* sp.) of *C. reniformis*, such differences in relative abundance within a minority portion of the community apparently do not suffice to

Table 4
THg levels in sponge fractions, associated microbiota, and seawater samples. The bioaccumulation factor (BAF) is also given. CrI = *Chondrosia reniformis* internal, referring to the choanosome; CrE = *C. reniformis* external, referring to the cortex.

Samples code	Sponge fraction (mg kg^{-1} d.w.)	Microbiome (mg kg^{-1} d.w.)	Filtered seawater (ng kg^{-1})	Water microbiome (mg kg^{-1} d.w.)	Unfiltered seawater (ng kg^{-1})*	BAF** ($x10^5$) in sponge fraction	BAF** ($x10^5$) in microbiota
CrI	0.70 ± 0.08 (0.51 – 0.82)	0.08 ± 0.01 (0.06 – 0.12)	3.3 ± 1.4	0.0034 $\pm$ 0.0008	3.9 ± 1.9	2.1 ± 0.3 (1.6 – 2.5)	0.25 ± 0.04 (0.19 – 0.37)
CrE	0.26 ± 0.07 (0.15 – 0.41)	0.079 ± 0.002 (0.068 – 0.12)				0.8 ± 0.2 (0.5 – 1.2)	0.25 ± 0.05 (0.19 – 0.35)

*Maximum Allowable Concentration 0.07 μg kg-1, established by the European Directive 2008/105/EC.
**Calculated using filtered seawater.

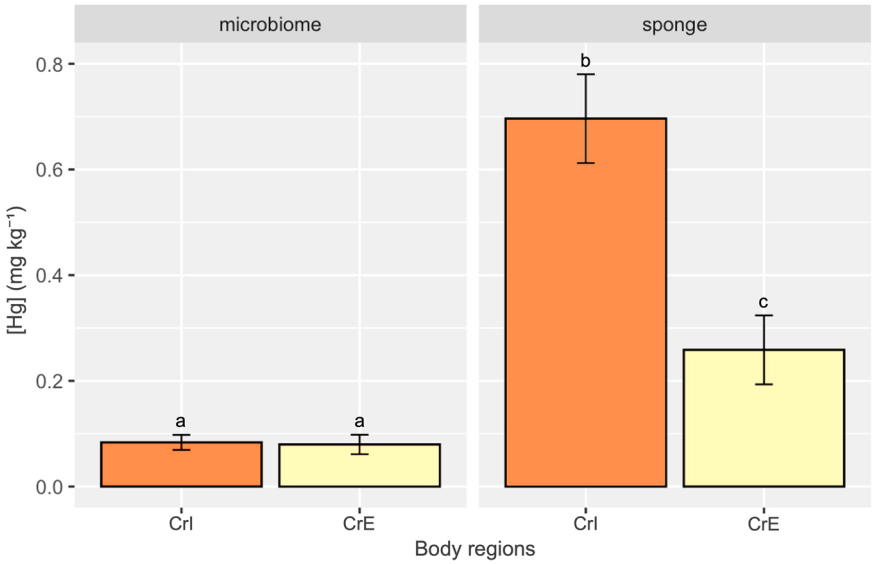

Fig. 4. Mean total mercury content (THg) (± standard deviation) detected in the microbial cells pellet ("microbiome") and the sponge fractions corresponding to the two body regions of *Chondrosia reniformis*. The different letters (a, b, c) indicate statistically significant differences in the THg content between groups (Dunn's test, $p < 0.05$; Tukey's test, $p < 0.05$). CrI = *C. reniformis* internal, referring to the choanosome; CrE = *C. reniformis* external, referring to the cortex.

trigger distinct, microbial-mediated Hg accumulation in the different body regions of the sponge host. Altogether, these results strengthen our current understanding of possible microbiome variability among specimens of the same sponge species (e.g., Schmitt et al., 2007, 2012; O'Connor-Sánchez et al., 2014; Slaby et al., 2017), as exposed above, and its implications to the accumulation of TEs in the marine environment. Notably, the microbiomes of sponges presenting a clear and strict separation between body regions (e.g., *Geodia* spp., *Stelletta* spp., *Chondrosia* spp. and others) have been seldom investigated, and the current study contributes to a better understanding of this issue.

Since *C. reniformis* is an HMA sponge (Ribes et al., 2012), its microbiota can reach high densities (10^8–10^{10} cells g^{-1} of sponge wet weight) and is presumably assembled by a blend of vertical and horizontal modes of symbiont transmission (Taylor et al., 2007). Microbial communities in HMA sponges are usually distinct in taxonomic composition from those of their surrounding environment (Hardoim et al., 2014; Thomas et al., 2016). These symbiotic consortia can actively participate in the metabolic cycles of their host, contributing with the biosynthesis of a multitude of inhibitory compounds, thus being considered as sources of novel metabolites with high biotechnological potential (Schmitt et al., 2007; Hentschel et al., 2012). In line with this notion, ordination analysis of zOTU profiles here performed enabled us to highlight several symbiont taxa enriched in *C. reniformis*, including the three ammonium-oxidizing archaea and bacteria (*C. symbiosum, N. maritimus* and *Nitrosococcus* sp.; Preston et al., 1996; Hallam et al., 2006; Feng et al., 2016), as well as *Acidobacteria* spp. and *Chloroflexi* spp., that may play important roles in nutrient cycling within this model organism. The selective enrichment of specific symbiont clades in *C. reniformis* was also reflected by the higher alpha-diversity measures observed in water with respect to the sponge, suggesting a host-driven selection of the symbiotic community, as reported also in other sponge species and marine invertebrates, such as corals (e.g., Karimi et al., 2017; Keller-Costa et al., 2017).

The enrichment of three ammonium-oxidizing lineages in *C. reniformis* (*C. symbiosum, N. maritimus* and *Nitrosococcus* sp.; Preston et al., 1996; Hallam et al., 2006; Feng et al., 2016) strongly suggests ammonia oxidation as a potential key metabolic pathway within the sponge. *C. symbiosum* and *N. maritimus* are, in fact, typical members of the microbiome of many sponges (e.g., Preston et al., 1996; Hallam et al., 2006; Feng et al., 2016), but are here identified for the first time in *C. reniformis*. However, their dominance in the total prokaryotic community of *C. reniformis* (composing up to the 7% and 25% of the dataset of both body regions, respectively) is not frequently reported in other studies on marine sponges, and thus can be considered a distinguishing feature of the symbiotic consortium in this host.

Similarly, important roles in carbon cycling may be played by Chloroflexi and *Nitrosococcus* spp. In fact, these bacterial taxa are abundant and widespread in HMA sponges (see e.g., Busch et al., 2020), and are usually involved in the process of CO_2 fixation (Jones and Morita, 1983; Zarzycki et al., 2009), but also participate in other central energy pathways, such as in the amino acid and fatty acid metabolism, respiration, tricarboxylic acid cycle, and pentose phosphate pathways (Klotz et al., 2006; Bayer et al., 2018).

Another example of an enriched bacterial phylum in *C. reniformis* is Acidobacteria, which appears to dominate the bacterial community of various HMA sponges (Hardoim and Costa, 2014; O'Connor-Sánchez et al., 2014; Slaby et al., 2017). However, information on their coding potential and physiology is still very scarce, since most of its members cannot be cultured and, in most studies, they have only been identified by their 16S rRNA gene sequences (O'Connor-Sánchez et al., 2014). Based on the construction of metagenome-assembled genomes, Slaby et al. (2017) suggested that representatives of this phylum evolved sophisticated mechanisms of defence against foreign DNA, since they present multiple restriction-modification and toxin-antitoxin systems, which are common attributes of obligate mutualists of marine sponges (Karimi et al., 2018). Future studies on Acidobacteria shall shed more light on the patterns of nutritional exchange between these symbionts and their sponge hosts.

Pseudomonas, one of the most abundant genera in our *C. reniformis* samples, is also a bacterial taxon well known to be involved in denitrification processes, presenting a variety of denitrifying genes (Jin et al., 2015; Feng and Li, 2019). In addition to various other microbial taxa, *Pseudomonas* spp. can also show high resistance to different TEs, being suggested as a suitable bioindicator for the monitoring of metal pollution in the marine environment (Selvin et al., 2009; Bauvais et al., 2015).

Samples of *C. reniformis* collected in Faro showed detectable concentrations of Hg, as also observed in the Mediterranean Sea (Perez et al., 2004; Roveta et al., 2020, 2022). This fact, along with the lack of variability in Hg content among samples of the same size, suggests this species as a potential bioindicator of Hg pollution. THg levels found in both cortex and choanosome were unequal, with higher concentrations

in the internal region, as already observed in the same species collected in the Tuscan Archipelago (Italy) by Roveta et al. (2022). A differentiated distribution of metals was also detected in the sponge *Spheciospongia vagabunda,* in which high Fe, Ni and Zn were distributed in patches or spots (Padovan et al., 2012). The distribution of the TEs within the sponge body is, in fact, often heterogeneous (Batista et al., 2014), and this phenomenon has been hypothesized to be correlated to different microbiota-mediated accumulation (Padovan et al., 2012), as demonstrated in other marine invertebrate taxa (i.e., ascidians) (Ueki et al., 2019). However, the THg concentrations found in *C. reniformis* microbiota extracted from the two body regions are similar, in line with the overall lack of differences found in the microbial community composition (see discussion above), suggesting that the same microbial species can accumulate Hg with the same rates. Therefore, in the considered sponge it is plausible that the higher Hg levels found in the internal region are not mediated by the microbiota. In fact, in *C. reniformis*, the water filtration takes place only in the choanosome, where choanocyte chambers are present (Bavestrello et al., 1988), and a polarization was seen in the incorporation of foreign matter, with the choanosome being not selective and able to incorporate every kind of material and compounds (Bavestrello et al., 1995, 1998a, 1998b; Cerrano et al., 1999), probably including metals.

Additionally, even though we cannot exclude the possibility that a residual portion of microorganisms are still present in the sponge fractions analysed for Hg content, the significantly lower Hg concentrations found in the microbial cell pellets suggest that alternative mechanisms might underlie the higher values observed in the sponge fractions. Since the method here applied allows to detect all the Hg present in the treated samples, Hg concentrations found in the sponge fraction can derive either from its cells, the extracellular matrix, or the collagen fibres. In fact, once metals enter in the sponge, they are generally bound by metallothioneins (i.e., cellular cysteine-rich metal-binding proteins), which can sequester metals and are involved in metal resistance and in the detoxification processes (Berthet et al., 2005; Roveta et al., 2021). Nonetheless, as demonstrated in the bath sponge *Spongia officinalis*, spongin fibres can present specific functional groups (e.g., C-C, C═C, C-OH, N-C═N, C-O-C, among others), able to bind Hg (see Domingues et al., 2021 for additional details), thus contributing to the bioaccumulation in the sponge. Therefore, considering the observed pattern of Hg distribution between the sponge and the microbial fractions, further studies on the actual histological location of Hg inside the sponge are needed to localize in which compartment *C. reniformis* stocks the metal.

The detectable concentration of Hg found in the microbiota can suggest a possible participation, at some level, of the microbial community in the bioaccumulation process. It is known that *Pseudomonas* and *Alteromonas* spp., isolated from the sponge *Fasciospongia cavernosa*, are resistant to Hg (Selvin et al., 2009), while, in different Brazilian sponges, various *Bacillus* and *Pseudomonas* strains presented the operon *mer* (A and B) in their genomes, which is involved in the mercury and methylmercury detoxification (Santos-Gandelman, 2014a, 2014b). Even though our study did not investigate the metal-resistance of microbes or the presence of the *mer* operon, all genera listed above are present in the prokaryotic community associated to *C. reniformis*. Therefore, our study lays the groundwork to further research on the possible involvement of the *C. reniformis* microbiome in Hg storage and detoxification, and to propose this species as a potentially suitable bioremediation tool in the Atlanto-Mediterranean area (Santos-Gandelman, 2014a, 2014b).

The only other study investigating the presence of TEs in the associated microbiome of a marine sponge was conducted by Keren et al. (2017) on the tropical species *Theonella swinhoei*. However, while the *C. reniformis* microbial fraction displayed lower Hg concentrations compared to the sponge fraction, Keren et al. (2017) found significantly higher As and Ba concentrations in the filamentous bacterium *Entotheonella* sp. (which dominates the microbiome of *T. swinhoei*) in comparison with the sponge fraction, while levels in unicellular bacteria and sponge cell fractions were similar (Keren et al., 2017). It is challenging to interpret the different patterns found between our study and that of Keren et al. (2017), but a few considerations can be proposed: (1) the analysed sponges belong to different species, and concentration of TEs can vary between taxa, from phyla down to species of the same genus (Rainbow, 2002); (2) the two sponges display a completely different microbial community, which can participate differently in the accumulation of TEs (for instance, *Entotheonella* sp. and *Cyanobacteria* seem to play an important role in As and Ba mineralization within *T. swinhoei*, but do not rank as abundant symbionts in *C. reniformis*) (Ueki et al., 2019); (3) different TEs were considered, and their bioaccumulation rates can vary depending on their nature (Simkiss and Taylor, 1995); (4) different protocols in the extraction of the microbiota were applied.

To conclude, our study represents the first detailed structural description of the prokaryotic communities associated to the two body regions of *C. reniformis*, and the first investigating the Hg content in the microbiome of a marine sponge. Finally, this work not only improves our current knowledge of the associated prokaryotic community of *C. reniformis*, but also establishes a baseline for future studies to deepen our understanding of the involvement of the microbiome and other components of the sponge (sponge cells, sponge matrix, exoskeleton) in the bioaccumulation and detoxification of mercury.

Funding

This research received financial support from the European Union's Horizon 2020 research and innovation programme, ASSEMBLE Plus Project [grant number 13130]; the Fundação para a Ciência e Tecnologia, I.P. (FCT) through structural funding to the Research Units Institute for Bioengineering and Biosciences - iBB [grant numbers UIDB/04565/2020, UIDP/04565/2020] and Associate Laboratory Institute for Health and Bioeconomy - i4HB [grant number LA/P/0140/2020].

Declaration of Competing Interest

The authors declare the following financial interests/personal relationships which may be considered as potential competing interests: Camilla Roveta reports financial support, administrative support, equipment, drugs, or supplies, and travel were provided by Europe Horizons. Rodrigo Costa reports financial support was provided by Fundação para a Ciência e Tecnologia.

Data availability

The zOTUs vs. samples tables used as input for alpha and beta diversity analysis performed in this study are available as a supplement to this article (Tables S3 and S4, Supplementary Material). Raw 16S rRNA gene sequences obtained for each sample were submitted to the European Nucleotide Archive under project accession number PRJEB57240 and run accession numbers ERR10464577-ERR10464587

Acknowledgements

Authors thank Carlos Afonso and Jorge M.S. Gonçalves from the Fisheries, Biodiversity and Conservation group and Nuno Padrão from the scientific diving centre at the Centro de Ciências do Mar (CCMAR) for logistical and technical support during sampling. We are also thankful to Marta Valente Bernardo for the assistance provided on DNA extraction and visualization procedures. We thank Tina Keller-Costa for providing support on data submission to public databases.

Appendix A. Supporting information

Supplementary data associated with this article can be found in the online version at doi:10.1016/j.zool.2023.126091.

References

Anderson, M.J., 2001. A new method for non-parametric multivariate analysis of variance. Austral. Ecol., 26(1), 32–46. https:// doi. org/ 10.1111/j. 1442- 9993. 2001. 01070.pp.x.

Anderson, M.J., Gorley, R.N., Clarke, K.R., 2008. PERMANOVA+ for PRIMER: Guide to Software and Statistical Methods. PRIMER-E, Plymouth Marine Laboratory, Plymouth, UK.

Apprill, A., McNally, S., Parsons, R., Weber, L., 2015. Minor revision to V4 region SSU rRNA 806R gene primer greatly increases detection of SAR11 bacterioplankton. Aquat. Microb. Ecol. 75 (2), 129–137. https://doi.org/10.3354/ame01753.

Batista, D., Muricy, G., Rocha, R.C., Miekeley, N.F., 2014. Marine sponges with contrasting life histories can be complementary biomonitors of heavy metal pollution in coastal ecosystems. Environ. Sci. Pollut. Res. 21 (9), 5785–5794. https://doi.org/10.1007/s11356-014-2530-7.

Bauvais, C., Zirah, S., Piette, L., Chaspoul, F., Domart-Coulon, I., Chapon, V., Gallice, P., Rebuffat, S., Pérez, T., Bourguet-Kondracki, M.L., 2015. Sponging up metals: bacteria associated with the marine sponge *Spongia officinalis*. Mar. Environ. Res. 104, 20–30. https://doi.org/10.1016/j.marenvres.2014.12.005.

Bavestrello, G., Burlando, B., Sara, M., 1988. The architecture of the canal systems of Petrosia ficiformis and *Chondrosia reniformis* studied by corrosion casts (Porifera, Demospongiae). Zoomorphology 108 (3), 161–166. https://doi.org/10.1007/BF00363932.

Bavestrello, G., Arillo, A., Calcinai, B., Cerrano, C., Lanza, S., Sara', M., Cattaneo-Vietti, R., Gaino, E., 1998a. Siliceous particles incorporation in *Chondrosia reniformis* (Porifera, Demospongiae). Ital. J. Zool. 65 (4), 343–348. https://doi.org/10.1080/11250009809386771.

Bavestrello, G., Arillo, A., Benatti, U., Cerrano, C., Cattaneo-Vietti, R., Cortesognoi, L., Gaggero, L., Giovine, M., Tonetti, M., Sarà, M., 1995. Quartz dissolution by the sponge *Chondrosia reniformis* (Porifera, Demospongiae). Nature 378 (6555), 374–376. https://doi.org/10.1038/378374a0.

Bavestrello, G., Benatti, U., Calcinai, B., Cattaneo-Vietti, R., Cerrano, C., Favre, A., Giovine, M., Lanza, S., Pronzato, R., Sarà, M., 1998b. Body polarity and mineral selectivity in the demosponge *Chondrosia reniformis*. Biol. Bull. 195 (2), 120–125. https://doi.org/10.2307/1542819.

Bayer, K., Jahn, M.T., Slaby, B.M., Moitinho-Silva, L., Hentschel, U., 2018. Marine sponges as *Chloroflexi* hot spots: genomic insights and high-resolution visualization of an abundant and diverse symbiotic clade. MSystems 3 (6), e00150-18. https://doi.org/10.1128/mSystems.00150-18.

Berthet, B., Mouneyrac, C., Pérez, T., Amiard-Triquet, C., 2005. Metallothionein concentration in sponges (*Spongia officinalis*) as a biomarker of metal contamination. Comp. Biochem. Physiol. Part C Toxicol. Pharmacol. 141 (3), 306–313. https://doi.org/10.1016/j.cca.2005.07.008.

Bonasoro, F., Wilkie, I.C., Bavestrello, G., Cerrano, C., Carnevali, M., 2001. Dynamic structure of the mesohyl in the sponge *Chondrosia reniformis* (Porifera, Demospongiae). Zoomorphology 121 (2), 109–121. https://doi.org/10.1007/PL00008497.

Busch, K., Wurz, E., Rapp, H.T., Bayer, K., Franke, A., Hentschel, U., 2020. Chloroflexi dominate the deep-sea golf ball sponges *Craniella zetlandica* and *Craniella infrequens* throughout different life stages. Front. Mar. Sci. 7, 674. https://doi.org/10.3389/fmars.2020.00674.

Cebrian, E., Uriz, M.J., Turon, X., 2007. Sponges as biomonitors of heavy metals in spatial and temporal surveys in northwestern Mediterranean: multispecies comparison. Environ. Toxicol. Chem. 26 (11), 2430–2439. https://doi.org/10.1897/07-292.1.

Cebrian, E., Agell, G., Martí, R., Uriz, M.J., 2006. Response of the Mediterranean sponge *Chondrosia reniformis* Nardo to copper pollution. Environ. Pollut. 141 (3), 452–458. https://doi.org/10.1016/j.envpol.2005.08.070.

Cerrano, C., Bavestrello, G., Benatti, U., Cattaneo-Vietti, R., Giovine, M., Sarà, M., 1999. Incorporation of inorganic matter into *Chondrosia reniformis* (Porifera, Demospongiae): the role of water turbolence. Mem. Qld. Mus. 44, 85–92.

Clarke, K.R., Gorley, R.N., 2015. Getting Started With PRIMER v7. PRIMER-E. Plymouth Marine Laboratory, Plymouth, UK.

Domingues, E.M., Gonçalves, G., Henriques, B., Pereira, E., Marques, P.A., 2021. High affinity of 3D spongin scaffold towards Hg (II) in real waters. J. Hazard. Mater. 407, 124807 https://doi.org/10.1016/j.jhazmat.2020.124807.

Easson, C.G., Chaves-Fonnegra, A., Thacker, R.W., Lopez, J.V., 2020. Host population genetics and biogeography structure the microbiome of the sponge *Cliona delitrix*. Ecol. Evol. 10 (4), 2007–2020. https://doi.org/10.1002/ece3.6033.

Edgar, R.C., 2010. Search and clustering orders of magnitude faster than BLAST. Bioinformatics 26 (19), 2460–2461. https://doi.org/10.1093/bioinformatics/btq461.

Edgar, R.C., Flyvbjerg, H., 2015. Error filtering, pair assembly and error correction for next-generation sequencing reads. Bioinformatics 31 (21), 3476–3482. https://doi.org/10.1093/bioinformatics/btv401.

Feng, G., Li, Z., 2019. Carbon and nitrogen metabolism of sponge microbiome. In: Li, Z. (Ed.), Symbiotic Microbiomes of Coral Reefs Sponges and Corals. Springer, Dordrecht, pp. 145–169. https://doi.org/10.1007/978-94-024-1612-1_9.

Feng, G., Sun, W., Zhang, F., Karthik, L., Li, Z., 2016. Inhabitancy of active *Nitrosopumilus*-like ammonia-oxidizing archaea and *Nitrospira* nitrite-oxidizing bacteria in the sponge *Theonella swinhoei*. Sci. Rep. 6 (1), 1–11. https://doi.org/10.1038/srep24966.

Fieseler, L., Quaiser, A., Schleper, C., Hentschel, U., 2006. Analysis of the first genome fragment from the marine sponge-associated, novel candidate phylum Poribacteria by environmental genomics. Environ. Microbiol. 8 (4), 612–624. https://doi.org/10.1111/j.1462-2920.2005.00937.x.

Fox, J., Weisberg, J., 2019. An (R) Companion to Applied Regression, third ed., Sage Publications, Thousand Oaks, CA. https://socialsciences.mcmaster.ca/jfox/Books/Companion/.

Gloeckner, V., Wehrl, M., Moitinho-Silva, L., Gernert, C., Schupp, P., Pawlik, J.R., Lindquist, N.L., Erpenbeck, D., Wörheide, G., Hentschel, U., 2014. The HMA-LMA dichotomy revisited: an electron microscopical survey of 56 sponge species. Biol. Bull. 227 (1), 78–88. https://doi.org/10.1086/BBLv227n1p78.

Griffiths, S.M., Antwis, R.E., Lenzi, L., Lucaci, A., Behringer, D.C., Butler IV, M.J., Preziosi, R.F., 2019. Host genetics and geography influence microbiome composition in the sponge *Ircinia campana*. J. Anim. Ecol. 88 (11), 1684–1695. https://doi.org/10.1111/1365-2656.13065.

Hallam, S.J., Konstantinidis, K.T., Putnam, N., Schleper, C., Watanabe, Y.I., Sugahara, J., Preston, C., de la Torre, J., Richardson, P.M., DeLong, E.F., 2006. Genomic analysis of the uncultivated marine crenarchaeote *Cenarchaeum symbiosum*. Proc. Natl. Acad. Sci. USA 103 (48), 18296–18301. https://doi.org/10.1073/pnas.0608549103.

Hammer, Ø., Harper, D.A.T., Ryan, P.D., 2001. PAST: Paleontological statistics software package for education and data analysis. Palaeontologia Electronica 4 (1), 9pp. http://palaeo-electronica.org/2001_1/past/issue1_01.htm..

Hardoim, C.C., Costa, R., 2014. Temporal dynamics of prokaryotic communities in the marine sponge *Sarcotragus spinosulus*. Mol. Ecol. 23 (12), 3097–3112. https://doi.org/10.1111/mec.12789.

Hardoim, C.C., Esteves, A.I., Pires, F.R., Gonçalves, J.M., Cox, C.J., Xavier, J.R., Costa, R., 2012. Phylogenetically and spatially close marine sponges harbour divergent bacterial communities. PLoS One 7 (12), e53029. https://doi.org/10.1371/journal.pone.0053029.

Hardoim, C.C., Cardinale, M., Cúcio, A.C., Esteves, A.I., Berg, G., Xavier, J.R., Cymon, J. C., Costa, R., 2014. Effects of sample handling and cultivation bias on the specificity of bacterial communities in keratose marine sponges. Front. Microbiol. 5, 611. https://doi.org/10.3389/fmicb.2014.00611.

Hentschel, U., Piel, J., Degnan, S.M., Taylor, M.W., 2012. Genomic insights into the marine sponge microbiome. Nat. Rev. Microbiol. 10 (9), 641–654. https://doi.org/10.1038/nrmicro2839.

Illuminati, S., Annibaldi, A., Truzzi, C., Scarponi, G., 2016. Heavy metal distribution in organic and siliceous marine sponge tissues measured by square wave anodic stripping voltammetry. Mar. Pollut. Bull. 111 (1–2), 476–482. https://doi.org/10.1016/j.marpolbul.2016.06.098.

Jin, R., Liu, T., Liu, G., Zhou, J., Huang, J., Wang, A., 2015. Simultaneous heterotrophic nitrification and aerobic denitrification by the marine origin bacterium *Pseudomonas* sp. ADN-42. Appl. Biochem. Biotechnol. 4, 2000–2011. https://doi.org/10.1007/s12010-014-1406-0.

Jones, R.D., Morita, R.Y., 1983. Methane oxidation by *Nitrosococcus oceanus* and *Nitrosomonas europaea*. Appl. Environ. Microbiol. 45 (2), 401–410. https://doi.org/10.1128/aem.45.2.401-410.1983.

Karimi, E., Ramos, M., Gonçalves, J., Xavier, J.R., Reis, M.P., Costa, R., 2017. Comparative metagenomics reveals the distinctive adaptive features of the *Spongia officinalis* endosymbiotic consortium. Front. Microbiol. 8, 2499. https://doi.org/10.3389/fmicb.2017.02499.

Karimi, E., Slaby, B.M., Soares, A.R., Blom, J., Hentschel, U., Costa, R., 2018. Metagenomic binning reveals versatile nutrient cycling and distinct adaptive features in alphaproteobacterial symbionts of marine sponges. FEMS Microbiol. Ecol. 94 (6), fiy074 https://doi.org/10.1093/femsec/fiy074.

Karimi, E., Keller-Costa, T., Slaby, B.M., Cox, C.J., da Rocha, U.N., Hentschel, U., Costa, R., 2019. Genomic blueprints of sponge-prokaryote symbiosis are shared by low abundant and cultivatable Alphaproteobacteria. Sci. Rep. 9 (1), 1–15. https://doi.org/10.1038/s41598-019-38737-x.

Kassambara, A., 2021. rstatix: Pipe-Friendly Framework for Basic Statistical Tests (R Package Version 0.7.0). ⟨https://CRAN.R-project.org/package=rstatix⟩.

Keller-Costa, T., Eriksson, D., Gonçalves, J.M., Gomes, N.C., Lago-Lestón, A., Costa, R., 2017. The gorgonian coral *Eunicella labiata* hosts a distinct prokaryotic consortium amenable to cultivation. FEMS Microbiol. Ecol. 93 (12) fix143. https://doi.org/10.1093/femsec/fix143.

Keren, R., Mayzel, B., Lavy, A., Polishchuk, I., Levy, D., Fakra, S.C., Pokroy, B., Ilan, M., 2017. Sponge-associated bacteria mineralize arsenic and barium on intracellular vesicles. Nat. Commun. 8 (1), 1–12. https://doi.org/10.1038/ncomms14393.

Klotz, M.G., Arp, D.J., Chain, P.S., El-Sheikh, A.F., Hauser, L.J., Hommes, N.G., et al., 2006. Complete genome sequence of the marine, chemolithoautotrophic, ammonia-oxidizing bacterium *Nitrosococcus oceani* ATCC 19707. Appl. Environ. Microbiol. 72 (9), 6299–6315. https://doi.org/10.1128/AEM.00463-06.

Lazoski, C., Solé-Cava, A., Boury-Esnault, N., Klautau, M., Russo, C., 2001. Cryptic speciation in a high gene flow scenario in the oviparous marine sponge *Chondrosia reniformis*. Mar. Biol. 139 (3), 421–429. https://doi.org/10.1007/s002270100542.

Li, M.L., Kwon, S.Y., Poulin, B.A., Tsui, M.T.K., Motta, L.C., Cho, M., 2022. Internal dynamics and metabolism of mercury in biota: a review of insights from mercury stable isotopes. Environ. Sci. Technol. 56 (13), 9182–9195. https://doi.org/10.1021/acs.est.1c08631.

Manz, W., Arp, G., Schumann-Kindel, G., Szewzyk, U., Reitner, J., 2000. Widefield deconvolution epifluorescence microscopy combined with fluorescence in situ hybridization reveals the spatial arrangement of bacteria in sponge tissue. J. Microbiol. Methods 40 (2), 125–134. https://doi.org/10.1016/S0167-7012(99)00103-7.

McMurdie, P.J., Holmes, S., 2013. phyloseq: an R package for reproducible interactive analysis and graphics of microbiome census data. PLoS One 8 (4), e61217. https://doi.org/10.1371/journal.pone.0061217.

Nyholm, S.V., McFall-Ngai, M., 2004. The winnowing: establishing the squid–vibrio symbiosis. Nat. Rev. Microbiol. 2 (8), 632–642. https://doi.org/10.1038/nrmicro957.

O'Connor-Sánchez, A., Rivera-Domínguez, A.J., los Santos-Briones, D., López-Aguiar, L. K., Peña-Ramírez, Y.J., Prieto-Davo, A., 2014. Acidobacteria appear to dominate the microbiome of two sympatric Caribbean Sponges and one Zoanthid. Biol. Res. 47 (1), 1–6. https://doi.org/10.1186/0717-6287-47-67.

Oksanen, J., Blanchet, F.G., Friendly, M., Kindt, R., Legendre, P., McGlinn, D., et al., 2020. *vegan*: Community Ecology Package. R. Package 2, 5–7 (Available online). ⟨https://CRAN.R-project.org/package=vegan⟩.

de Oliveira, B.F.R., Freitas-Silva, J., Sánchez-Robinet, C., Laport, M.S., 2020. Transmission of the sponge microbiome: moving towards a unified model. Environ. Microbiol. Rep. 12 (6), 619–638. https://doi.org/10.1111/1758-2229.12896.

Orani, A.M., Vassileva, E., Azemard, S., Thomas, O.P., 2020. Comparative study on Hg bioaccumulation and biotransformation in Mediterranean and Atlantic sponge species. Chemosphere 260, 127515. https://doi.org/10.1016/j.chemosphere.2020.127515.

Padovan, A., Munksgaard, N., Alvarez, B., McGuinness, K., Parry, D., Gibb, K., 2012. Trace metal concentrations in the tropical sponge *Spheciospongia vagabunda* at a sewage outfall: synchrotron X-ray imaging reveals the micron-scale distribution of accumulated metals. Hydrobiologia 687, 275–288. https://doi.org/10.1007/978-94-007-4688-6_23.

Parada, A.E., Needham, D.M., Fuhrman, J.A., 2016. Every base matters: assessing small subunit rRNA primers for marine microbiomes with mock communities, time series and global field samples. Environ. Microbiol. 18 (5), 1403–1414. https://doi.org/10.1111/1462-2920.13023.

Perez, T., Vacelet, J., Rebouillon, P., 2004. In situ comparative study of several Mediterranean sponges as potential biomonitors of heavy metals. In: Pansini, M., Pronzato, R., Bavestrello, G., Manconi, R. (Eds.), Sponge Science in the New Millennium. Officine Grafiche Canessa Rapallo, Genova, Italy, pp. 517–525.

Perez, T., Longet, D., Schembri, T., Rebouillon, P., Vacelet, J., 2005. Effects of 12 years' operation of a sewage treatment plant on trace metal occurrence within a Mediterranean commercial sponge (*Spongia officinalis*, Demospongiae). Mar. Pollut. Bull. 50 (3), 301–309. https://doi.org/10.1016/j.marpolbul.2004.11.001.

Pozzolini, M., Scarfì, S., Mussino, F., Ferrando, S., Gallus, L., Giovine, M., 2015. Molecular cloning, characterization, and expression analysis of a prolyl 4-hydroxylase from the marine sponge *Chondrosia reniformis*. Mar. Biotechnol. 17 (4), 393–407. https://doi.org/10.1007/s10126-015-9630-3.

Pozzolini, M., Bruzzone, F., Berilli, V., Mussino, F., Cerrano, C., Benatti, U., Giovine, M., 2012. Molecular characterization of a nonfibrillar collagen from the marine sponge *Chondrosia reniformis* Nardo 1847 and positive effects of soluble silicates on its expression. Mar. Biotechnol. 14 (3), 281–293. https://doi.org/10.1007/s10126-011-9415-2.

Pozzolini, M., Scarfì, S., Ghignone, S., Mussino, F., Vezzulli, L., Cerrano, C., Giovine, M., 2016. Molecular characterization and expression analysis of the first Porifera tumor necrosis factor superfamily member and of its putative receptor in the marine sponge *Chondrosia reniformis*. Dev. Comp. Immunol. 57, 88–98. https://doi.org/10.1016/j.dci.2015.12.011.

Pozzolini, M., Scarfì, S., Gallus, L., Castellano, M., Vicini, S., Cortese, K., Gagliani, M.C., Bertolino, M., Costa, G., Giovine, M., 2018. Production, characterization and biocompatibility evaluation of collagen membranes derived from marine sponge *Chondrosia reniformis* Nardo, 1847. Mar. Drugs 16 (4), 111. https://doi.org/10.3390/md16040111.

Preston, C.M., Wu, K.Y., Molinski, T.F., DeLong, E.F., 1996. A psychrophilic crenarchaeon inhabits a marine sponge: *Cenarchaeum symbiosum* gen. nov., sp. nov. Proc. Natl. Acad. Sci. USA 93 (13), 6241–6246. https://doi.org/10.1073/pnas.93.13.6241.

R Core Team, 2021. R: a Language and Environment for Statistical Computing, R Foundation for Statistical Computing, Vienna, Austria. https://www.R-project.org/.

Rainbow, P.S., 2002. Trace metal concentrations in aquatic invertebrates: why and so what. Environ. Pollut. 120 (3), 497–507. https://doi.org/10.1016/S0269-7491(02)00238-5.

Ribes, M., Jiménez, E., Yahel, G., López-Sendino, P., Díez, B., Massana, R., Sharp, J.H., Coma, R., 2012. Functional convergence of microbes associated with temperate marine sponges. Environ. Microbiol. 14 (5), 1224–1239. https://doi.org/10.1111/j.1462-2920.2012.02701.x.

Rodriguez Jimenez, A., Dechamps, E., Giaux, A., Goetghebuer, L., Bauwens, M., Willenz, P., Flahaut, S., Laport, M.S., George, I.F., 2021. The sponges *Hymeniacidon perlevis* and *Halichondria panicea* are reservoirs of antibiotic-producing bacteria against multi-drug resistant Staphylococcus aureus. J. Appl. Microbiol. 131 (2), 706–718. https://doi.org/10.1111/jam.14999.

Roveta, C., Pica, D., Calcinai, B., Girolametti, F., Truzzi, C., Illuminati, S., Annibaldi, A., Puce, S., 2020. Hg levels in marine Porifera of Montecristo and Giglio Islands (Tuscan Archipelago, Italy. Appl. Sci. 10 (12), 4342. https://doi.org/10.3390/app10124342.

Roveta, C., Annibaldi, A., Calcinai, B., Girolametti, F., Illuminati, S., Mantas, T.P., Truzzi, C., Puce, S., 2021. Biomonitoring of Heavy Metals: The Unexplored Role of Marine Sessile Taxa. Appl. Sci. 11 (2), 508. https://doi.org/10.3390/app11020580.

Roveta, C., Annibaldi, A., Calcinai, B., Girolametti, F., Illuminati, S., Mantas, T.P., Truzzi, C., Puce, S., 2022. Distribution of mercury inside the Mediterranean sponge *Chondrosia reniformis*: a study case from the Tuscan Archipelago National Park (Tyrrhenian Sea). J. Sea Res. 184, 102206 https://doi.org/10.1016/j.seares.2022.102206.

Santos-Gandelman, J.F., Giambiagi-deMarval, M., Muricy, G., Barkay, T., Laport, M.S., 2014a. Mercury and methylmercury detoxification potential by sponge-associated bacteria. Antonie Van. Leeuwenhoek 106 (3), 585–590. https://doi.org/10.1007/s10482-014-0224-2.

Santos-Gandelman, J.F., Cruz, K., Crane, S., Muricy, G., Giambiagi-deMarval, M., Barkay, T., Laport, M.S., 2014b. Potential application in mercury bioremediation of a marine sponge-isolated Bacillus cereus strain Pj1. Curr. Microbiol. 69 (3), 374–380. https://doi.org/10.1007/s00284-014-0597-5.

Scarfì, S., Pozzolini, M., Oliveri, C., Mirata, S., Salis, A., Damonte, G., Fenoglio, D., Altosole, T., Ilan, M., Bertolino, M., Giovine, M., 2020. Identification, purification and molecular characterization of chondrosin, a New Protein with anti-tumoral activity from the marine sponge *Chondrosia reniformis* nardo 1847. Mar. Drugs 18 (8), 409. https://doi.org/10.3390/md18080409.

Schmitt, S., Wehrl, M., Siegl, A., Hentschel, U., 2007. Marine sponges as models for commensal microbe-host interactions. Symbiosis 44, 43–50.

Schmitt, S., Tsai, P., Bell, J., Fromont, J., Ilan, M., Lindquist, N., Pérez, T., Rodrigo, A., Schupp, P.J., Vacelet, J., Webster, N., Hentschel, U., Taylor, M.W., 2012. Assessing the complex sponge microbiota: core, variable and species-specific bacterial communities in marine sponges. ISME J. 6 (3), 564–576. https://doi.org/10.1038/ismej.2011.116.

Selvin, J., Priya, S.S., Kiran, G.S., Thangavelu, T., Bai, N.S., 2009. Sponge-associated marine bacteria as indicators of heavy metal pollution. Microbiol. Res. 164 (3), 352–363. https://doi.org/10.1016/j.micres.2007.05.005.

Simkiss, K., Taylor, M.G., 1995. Transport of metals across membranes. In: Tessier, A., Turner, D. (Eds.), Metal Speciation and Bioavailability in Aquatic Systems. John Wiley & Sons Ltd, Chichester, UK, pp. 1–44. https://doi.org/10.1038/s43705-021-00007-1.

Slaby, B.M., Hackl, T., Horn, H., Bayer, K., Hentschel, U., 2017. Metagenomic binning of a marine sponge microbiome reveals unity in defense but metabolic specialization. ISME J. 11 (11), 2465–2478. https://doi.org/10.1038/ismej.2017.101.

Taylor, M.W., Radax, R., Steger, D., Wagner, M., 2007. Sponge-associated microorganisms: evolution, ecology, and biotechnological potential. Microbiol. Mol. Biol. Rev. 71 (2), 295–347. https://doi.org/10.1128/MMBR.00040-06.

Thomas, T., Moitinho-Silva, L., Lurgi, M., Björk, J.R., Easson, C., Astudillo-García, C., Olson, J.B., Erwin, P.M., López-Legentil, S., Luter, H., Chaves-Fonnegra, A., Costa, R., Shupp, P.J., Steindler, L., Erpenbeck, D., Gilbert, J., Knight, R., Ackermann, G., Victor Lopez, J., Taylor, M.W., Thacker, R.W., Montoya, J.M., Hentschel, U., Webster, N.S., 2016. Diversity, structure and convergent evolution of the global sponge microbiome. Nat. Commun. 7 (1), 1–12. https://doi.org/10.1038/ncomms11870.

Thompson, A.W., Ward, A.C., Sweeney, C.P., Sutherland, K.R., 2021. Host-specific symbioses and the microbial prey of a pelagic tunicate (*Pyrosoma atlanticum*). ISME Commun. 1 (1), 1–10.

Ueki, T., Fujie, M., Satoh, N., 2019. Symbiotic bacteria associated with ascidian vanadium accumulation identified by 16S rRNA amplicon sequencing. Mar. Genom. 43, 33–42. https://doi.org/10.1016/j.margen.2018.10.006.

Vacelet, J., Donadey, C., 1977. Electron microscope study of the association between some sponges and bacteria. J. Exp. Mar. Biol. Ecol. 30 (3), 301–314. https://doi.org/10.1016/0022-0981(77)90038-7.

Versluis, D., Rodriguez de Evgrafov, M., Sommer, M.O., Sipkema, D., Smidt, H., Van Passel, M.W., 2016. Sponge microbiota are a reservoir of functional antibiotic resistance genes. Front. Microbiol., 7, 1848. https://doi.org/10.3389/fmicb.2016.01848.

Webster, N.S., Luter, H.M., Soo, R.M., Botté, E.S., Simister, R.L., Abdo, D., Whalan, S., 2013. Same, same but different: symbiotic bacterial associations in GBR sponges. Front. Microbiol. 3, 444. https://doi.org/10.3389/fmicb.2012.00444.

Weisz, J.B., Lindquist, N., Martens, C.S., 2008. Do associated microbial abundances impact marine demosponge pumping rates and tissue densities. Oecologia 155, 367–376. https://doi.org/10.1007/s00442-007-0910-0.

Wickham, H., 2011. The split-apply-combine strategy for data analysis. J. Stat. Softw. 40 (1), 1–29. https://doi.org/10.18637/jss.v040.i01.

Wickham, H., 2016. ggplot2: Elegant Graphics for Data Analysis, Springer International Publishing, New York, NY.

Wilkinson, C.R., Vacelet, J., 1979. Transplantation of marine sponges to different conditions of light and current. J. Exp. Mar. Biol. Ecol. 37 (1), 91–104. https://doi.org/10.1016/0022-0981(79)90028-5.

Zarzycki, J., Brecht, V., Müller, M., Fuchs, G., 2009. Identifying the missing steps of the autotrophic 3-hydroxypropionate CO_2 fixation cycle in *Chloroflexus aurantiacus*. Proc. Natl. Acad. Sci. USA 106 (50), 21317–21322. https://doi.org/10.1073/pnas.0908356106.